Progress In Electromagnetics Research C, Vol. 77, 145–153, 2017

A Novel Frequency Reconfigurable Monopole Antenna with Switchable Characteristics between Band-Notched UWB and WLAN Applications

Dinesh Yadav[1, *], Mahesh P. Abegaonkar[2], Shiban K. Koul[2], Vivekanand Tiwari[1], and Deepak Bhatnagar[3]

Abstract—This paper presents a novel frequency reconfigurable monopole antenna that has switchable notch characteristic at center frequency of 5.3 GHz. The proposed antenna consists of a defective ground structure (DGS) to enhance the impedance bandwidth from 3.17 to 13 GHz. The F-shaped parasitic element with three stubs (two vertical and one horizontal) are located on the back side of the radiating patch to achieve the band rejection characteristics from 4.9 GHz to 5.7 GHz. The metallic ground plane structure is connected or disconnected to the F-shaped parasitic element through stubs by means of p-i-n diodes. Experimental demonstration of applications of the proposed antenna structure as 5.3 GHz notched band ultra-wideband (UWB) antenna with all diodes in the OFF-state and as 5.3 GHz radiator for wireless local area network (WLAN) with all diodes in the ON-state is reported. In both the cases, good agreements between measured and simulated return losses, radiation patterns and realized gains are observed.

1. INTRODUCTION

Ultra-wideband (UWB) monopole antennas are the most promising solution for communication systems due to their low profile, low cost, light weight, ease of fabrication, wide impedance bandwidth, simple structure and flexibility of integration with other microstrip circuits. The Federal Communications Commission (FCC) has allocated an unlicensed band that ranges from 3.1 to 10.6 GHz that produces a low equivalent isotropically radiated power (EIRP) of −41.3 dBm [1]. However, other narrowband systems, such as Wi-MAX (3.4–3.69 GHz), IEEE 802.11a WLAN (5.15–5.35 GHz, 5.725–5.825 GHz) and HIPERLAN (5.45–5.725 GHz), generally affect the UWB system in terms of signal interference. In order to overcome the problems related to signal interference, band-notched UWB antennas are required and hence, are frequently used due to their ability to utilize the complete spectrum in the absence of interfering signals in its close proximity [2].

In recent years, it is observed that frequency reconfigurable radiators are widely used with wireless devices due to ease of switching to a desired resonant frequency for operation over multi-serviced radio spectrum [3, 4]. Structures that combine two independent antennas operating in different frequency bands with a single feed and able to perform efficient switching and tuning between two or more operating bands have been widely discussed [5–8]. For minimizing the interference between narrow band and UWB systems, several types of printed antennas with reconfigurable band notch characteristics have also been proposed in the literature [9–11]. Some studies also highlight the use of p-i-n diode, varactor diode and RF micro-electromechanical system (MEMS) switches towards the design of reconfigurable

Received 22 June 2017, Accepted 17 August 2017, Scheduled 31 August 2017

* Corresponding author: Dinesh Yadav (dineshyadav_1984@yahoo.co.in).

[1] Department of Electronics & Communication Engineering, Manipal University Jaipur, Rajasthan, India. [2] Centre for Applied Research in Electronics (CARE), Indian Institute of Technology (IIT) Delhi, Hauz Khas, New Delhi, India. [3] Microwave Lab, Department of Physics, University of Rajasthan, India.

printed antennas that are able to switch between available spectrums besides providing complete coverage within UWB and band-notched UWB of the single/dual tunable bands [9–13]. The use of switchable and tunable notch in UWB filter incorporating a total of sixteen p-i-n diodes connected in parallel has also been proposed by some researchers [14].

In this communication, a novel frequency reconfigurable monopole antenna with switchable notch characteristics between UWB and WLAN is presented. The proposed antenna is capable to switch between 5.3 GHz notched-band UWB antenna to 5.3 GHz WLAN antenna. The proposed antenna structure utilizes an F-shape parasitic element with three stubs connected and disconnected with metallic ground plane using p-i-n diodes to form the reconfigurable structure.

2. ANTENNA DESIGN AND ANALYSIS

2.1. Basic Monopole UWB Antenna Design

The design of the proposed antenna structure was initiated with the consideration of monopole UWB antenna having the overall size of antenna as $22 \times 29\,\text{mm}^2$, as shown in Fig. 1(a). The proposed antenna structure is located on the x-y plane, and its normal direction is parallel to the z-axis. The antenna is designed on an FR-4 glass epoxy substrate (dielectric constant $\epsilon_r = 4.3$ and loss tangent $\tan\delta = 0.025$) with thickness of the substrate $d = 1.6\,\text{mm}$ and fed by a 50-Ω microstrip line. The optimized length of the feed line is fixed at 6 mm. The gap 'g' between the rectangular patch and ground is 0.5 mm. To achieve 50-Ω impedance, the width of the feed line 'W_f' is calculated according to [15]. The lower cutoff frequency of the rectangular monopole UWB microstrip radiator corresponds to VSWR < 2 calculated using [16]. For the patch dimensions, length of the patch $L_P = 16.5\,\text{mm}$, width of the patch $W_P = 11.5\,\text{mm}$ and ground-patch gap $g = 0.5\,\text{mm}$, the calculated value of lower cutoff frequency is 3.82 GHz. The size of the designed rectangular patch is $16.5 \times 11.5\,\text{mm}^2$. The optimum value of the ground length is 5.5 mm, and width of the ground is equal to the width of the substrate. After simulating and optimizing antenna configuration without DGS for maximum impedance bandwidth using Computer Simulation Technology (CST) Microwave studio simulator [17], it is observed that the impedance bandwidth (reflection coefficient $< -10\,\text{dB}$) is 8.04 GHz (3.55 to 11.59 GHz). The dimensions of the basic monopole UWB antenna after optimization are as follows: $L_s = 22\,\text{mm}$, $W_s = 29\,\text{mm}$, $L_p = 16.5\,\text{mm}$, $W_p = 11.5\,\text{mm}$, $W_f = 2.8\,\text{mm}$, $L_f = 6\,\text{mm}$, $L_g = 5.5\,\text{mm}$, $g = 0.5\,\text{mm}$, $W_r = 6.1\,\text{mm}$, $W_g = 4.25\,\text{mm}$, $d = 1.6\,\text{mm}$, $d_1 = 4.5\,\text{mm}$, $d_2 = 18.5\,\text{mm}$, $h_1 = 1\,\text{mm}$, $h_2 = 4\,\text{mm}$, $v = 0.25\,\text{mm}$.

The next task is to further improve the impedance bandwidth and minimize the lower cutoff frequency by introducing DGS technique. In [18], two V-shaped slots are inserted in the ground plane structure to provide one more resonance, and two more resonances have been discussed. The impedance bandwidth enhancement with rectangular, circular and fractal DGSs has also been proposed in [19].

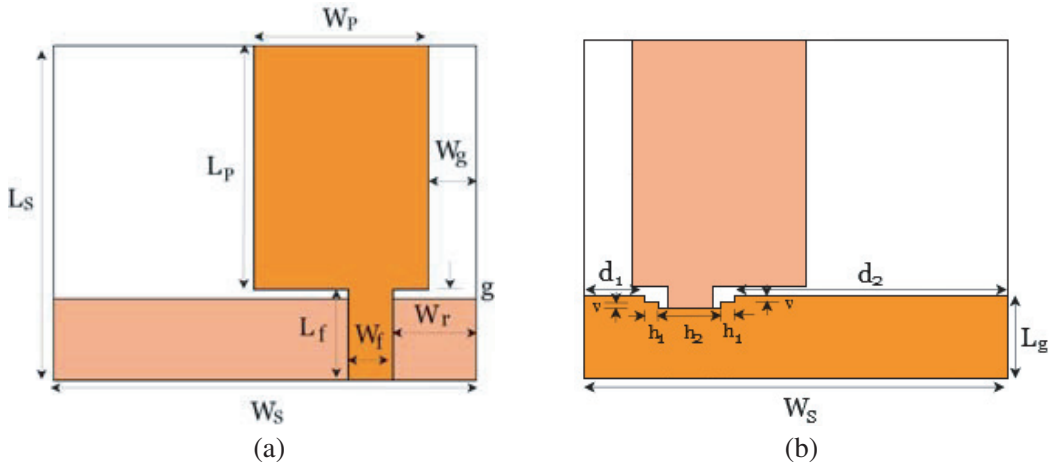

Figure 1. UWB monopole antenna structure, (a) front view without DGS, (b) back view with DGS.

In order to improve impedance bandwidth, the upper edge of the ground plane is shaped using two rectangular slots of size $0.25 \times 6\,\text{mm}^2$ and $0.25 \times 4\,\text{mm}^2$ as shown in Fig. 1(b). The vertical path on the rectangular slot is shown by 'v', and the horizontal paths are shown by 'h_1' and 'h_2'. The width of the designed upper rectangular slot is $h_1 + h_2 + h_1 = 6\,\text{mm}$, and length is $v = 0.25\,\text{mm}$. Similarly, the width of the designed lower rectangular slot is $h_2 = 4\,\text{mm}$, and length is the same as that of upper rectangular slot.

The surface current path to the upper edge of the ground plane without DGS is $W_s = 29\,\text{mm}$, whereas with DGS is $W_s + 4 \times v = 30\,\text{mm}$. It can be seen that the surface current path to the upper edge of the ground plane is increased by 1 mm with DGS [17]. The current distribution on the rectangular slotted ground plane affects the impedance bandwidth of the antenna. The two rectangular slots in ground plane structure provide additional resonance at lower and higher cutoff frequencies. As a result, the impedance bandwidth is improved, and the lower cutoff frequency is shifted to 3.17 GHz. As illustrated in Fig. 2, the UWB antenna with slotted ground plane has a wider impedance bandwidth than the same antenna without slots in the ground plane. The simulated results indicate a wider impedance bandwidth ranging from 3.17 GHz to more than 12 GHz with DGS.

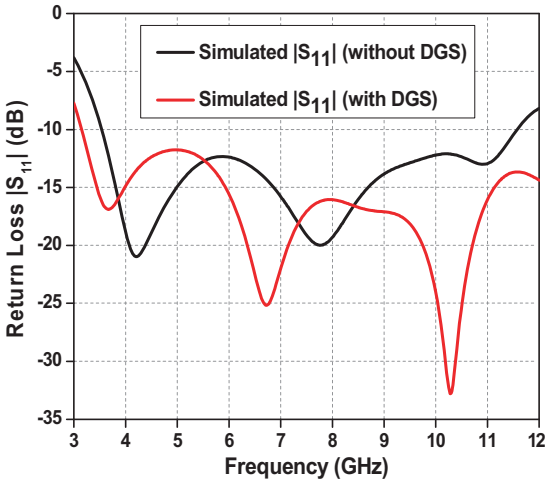

Figure 2. Simulated return loss plot with and without DGS.

2.2. Reconfigurable Monopole Antenna with Switchable Notch Characteristics

The next step is to achieve the band-notched characteristics for the UWB antenna. The purpose is to design band-notched UWB antennas to overcome the narrow band interference with the UWB impedance bandwidth. The back view of the proposed reconfigurable UWB antenna with dimensions is shown in Fig. 3(a). The ground plane consists of a horizontal F-shaped parasitic element with three stubs (one horizontal and two vertical). The return loss characteristics with variation in different ground plane parameters are exhibited in Figs. 4(a)–(c). It is observed that by varying ground plane parameters of the F-shaped parasitic element: the length of the stub (L_1), length of the stub (L_2) and width of the stub (t_2). The bandwidth and center of the notched band can be controlled. The sizes of the vertical and horizontal stubs, which are disconnected with the F-shaped parasitic element are $3.15 \times 1\,\text{mm}^2$ and $1 \times 5.7\,\text{mm}^2$, respectively. Five MA-COM p-i-n diodes (MA4SPS402) are used as switches between the gaps $G = 0.3\,\text{mm}$. Five inductors of 30-nH are used as RF chokes in the bias circuitry. The additional optimized dimensions of the ground plane structure are as follows: $W_1 = 12\,\text{mm}$, $W_2 = 4\,\text{mm}$, $W_3 = 5.7\,\text{mm}$, $W_4 = 2\,\text{mm}$, $G = 0.3\,\text{mm}$, $l_1 = 6.8\,\text{mm}$, $l_2 = 10\,\text{mm}$, $l_3 = l_4 = 3.15\,\text{mm}$, $t_1 = t_4 = 1\,\text{mm}$, $t_2 = t_3 = 2\,\text{mm}$, $s = 0.5\,\text{mm}$. The antenna structure with five 30-nH inductors used as RF chokes in the bias circuitry and five p-i-n diodes is shown in Fig. 3(b). Figs. 5(a)–(b) show the return loss plots at different diode states. In order to minimize the number of diodes, first two return loss plots of Fig. 5(a) show that the diodes (D_2 and D_4) are in ON state which indicates that lower edges of the vertical stubs are always connected with ground plane. As a result, the surface current path of the

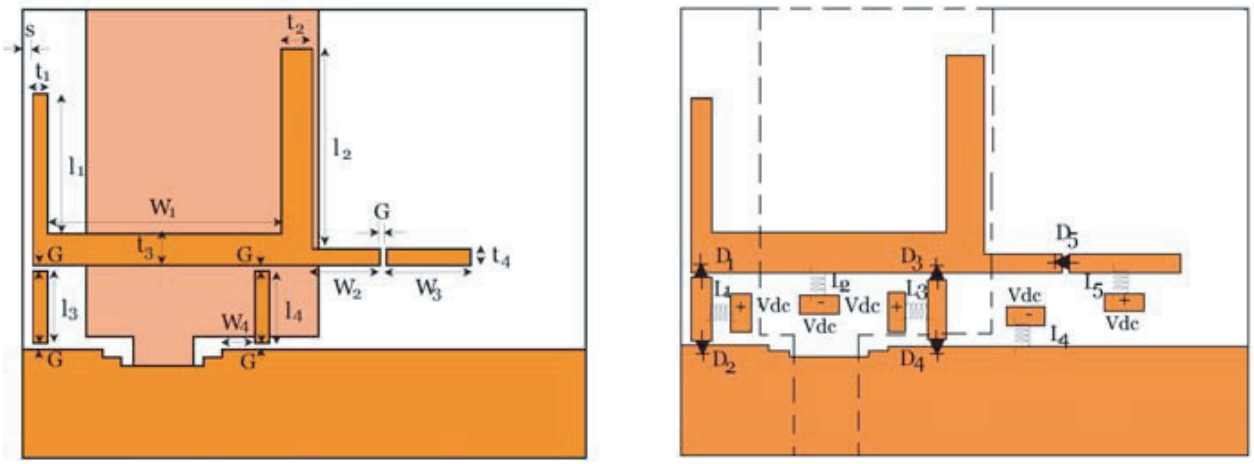

(a) (b)

Figure 3. Back view of the proposed antenna structure, (a) with dimensions, (b) with biased circuitry.

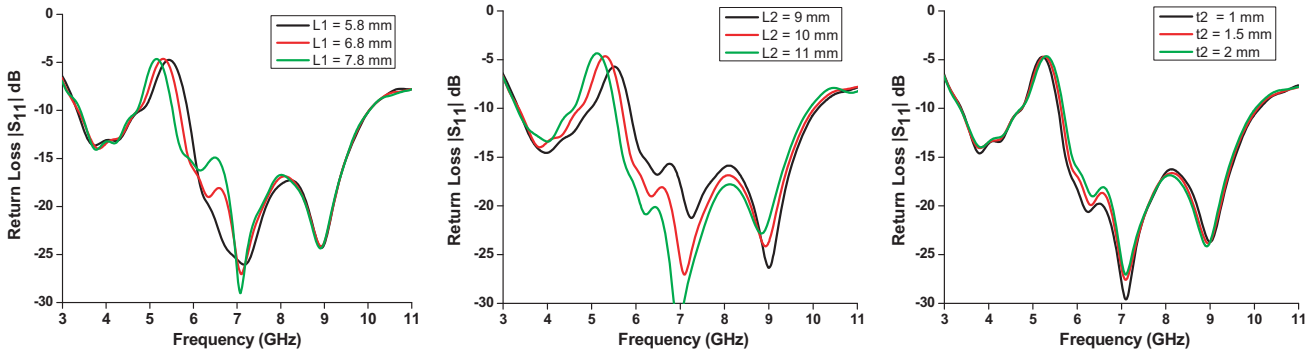

(a) (b) (c)

Figure 4. Simulated return loss with variation in ground structure parameters, (a) stub length L_1, (b) stub length L_2 and (c) stub width t_2.

upper edge of the ground plane is increased, discussed in Section 2.1. In this case, the resonance of the reconfigurable structure switching is due to bias state of the other three diodes, which is illustrated in first two results of Fig. 5(a). Similarly, if diodes (D_1 and D_3) are in ON state, the upper edge of the vertical stubs are always connected with the F-shaped parasitic element. As a result, the overall length of the F-shaped parasitic element is increased, which is designed for the 5.3 GHz notched frequency band. On the bases of the biases state of remaining three diodes, the return loss plots are shown in Fig. 5(a). In conclusion, when the vertical stubs are not connected with F-shaped parasitic stub and ground plane, only 5.3 GHz band notched UWB antenna characteristics can be achieved. Further, to switch the resonance in 5.3 GHz radiation with four diodes (D_1 to D_4) in ON-state, it is observed from Fig. 5(b) that additional resonance is generated at 3.6 GHz with 5.3 GHz, having diode (D_5) in the OFF state. With diode (D_5) in the ON-state, the horizontal stub is now connected with ground plane and F-shaped parasitic element, which increases the total length of the ground plane elements. As a result, with all diodes in the ON-state, the maximum surface current at 3.6 GHz is concentrated around the horizontal stub, and radiation occurs only at 5.3 GHz as depicted in Fig. 5(b).

The prototype of the proposed antenna is fabricated on an FR-4 substrate, which is connected to a 50-Ω SMA connector for signal transmission. The front and back views of the fabricated prototype are shown in Figs. 6(a) and (b), respectively. Fig. 6(c) shows the zoomed view of the reconfigurable section having five p-i-n diodes (D_1 to D_5) and five inductors circuitry in a combination of three stubs with parasitic element to connect or disconnect from the ground plane structure.

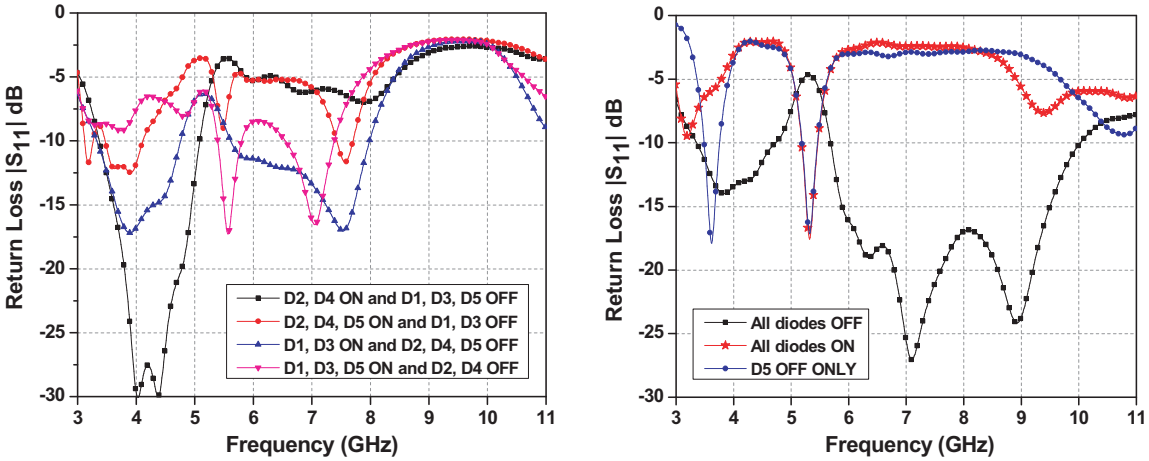

Figure 5. Simulated return loss plot of proposed antenna with different diode states.

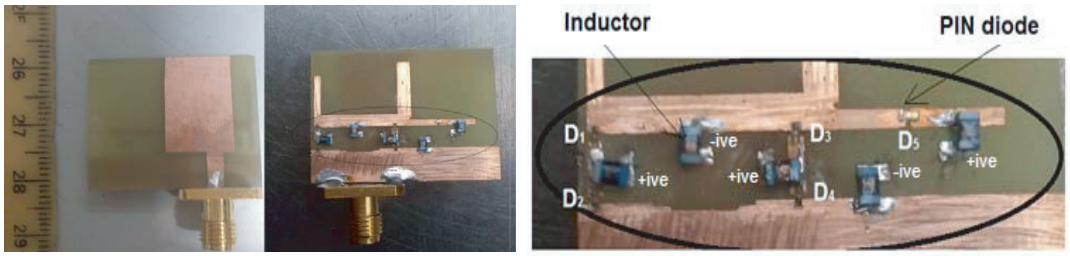

Figure 6. Photograph of the proposed antenna, (a) front view, (b) back view, (c) zoomed view of the reconfigurable section.

3. RESULTS AND DISCUSSIONS

The proposed antenna is printed on a 1.6-mm-thick FR-4 substrate of relative dielectric constant 4.3 and loss tangent 0.025. The return loss measurements are carried out using Anritsu MS2028C vector network analyzer. In ground structure, five p-i-n diodes are connected in between the gap 'G' which was modelled as a 0.1 Ω resistance for the ON-state, and a 0.045-pF capacitance parallel with a 20-kΩ resistance in the OFF-state. The p-i-n diode has lower parasitic inductance (0.45-nH) and excellent 'RC' constant (0.23-pS), which make it ideal for higher frequency switches. The size of this diode is very small (1290 µm × 533 µm), and the manufacturer recommends thermo-compression bonding to mount it on the PCB [20].

The equivalent electrical model of single p-i-n diode is modelled in ADS (Advanced Design Software), and the behaviors of the diode at higher frequencies are observed. The return loss and transmission coefficient of the single p-i-n diode model at zero or reverse bias are also studied. It is observed that at zero bias or reverse bias voltage ($V_r = -5$ V or -10 V), the magnitude of the return loss is greater than -10 dB, and transmission coefficient is less than -10 dB at entire frequency band up to 13 GHz. The reason is that under reverse bias voltage condition, the values of 'R_p' parallel resistance and 'C_T' parallel capacitance increase with frequency increment, and device behaves as an open circuit switch. At forward bias voltage ($V_f = 0.75$ V to 0.9 V), the forward current varies from 10 mA to 50 mA, and 'R_s' series resistance decreases with frequency increment. As a result, the magnitude of the return loss is less than -10 dB; transmission coefficient is greater than -10 dB; device behave as a short circuit switch. The return loss and transmission coefficient of the single p-i-n diode model with forward bias current for whole UWB band are also achieved.

To simulate the structure with all the diodes in the ON-state, five metallic strips of the size (0.5 mm × 0.2 mm) are placed to connect stubs with ground plane and F-shaped parasitic element in the CST microwave studio. By eliminating the metallic strips, the simulation of the structure is achieved when all the diodes are in the OFF-state. Moreover, to analyze the loading of diodes and inductors on antenna structure, initially full-wave simulation of the antenna is done with one discrete port in the place of each diode and each inductor along with input in CST. The simulated S-parameter file with discrete ports is then imported into ADS for circuit modelling. The diode model and *S*-parameter file of the inductors are used to complete the simulation setup in the ADS. The simulated and measured return losses with OFF-states of the diodes are shown in Fig. 7(a). It can be observed that the simulated operating bands of the antenna, 3.3 to 4.9 GHz and 5.7 to 10.3 GHz with 4.9 to 5.7 GHz band-notched frequency, have good agreement for both simulation tools. The measured operating bands of the proposed antenna are 3.5 to 4.9 GHz and 6 to 10.3 GHz with 4.9 to 6 GHz band-notched frequency. As observed, satisfactory agreement has been obtained between simulated and measured results.

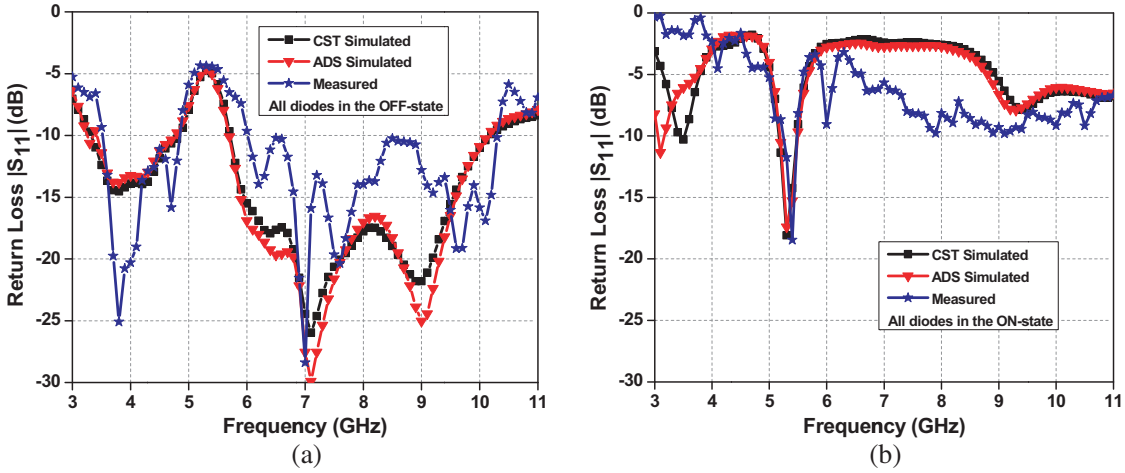

Figure 7. Measured and simulated return loss plot of proposed antenna, (a) with all the diodes in the OFF-state, (b) with all the diodes in the ON-state.

When all the p-i-n diodes are turned ON with a single power supply having total source current of 50-mA, the F-shaped parasitic element is shorted to the ground plane and the horizontal stub. In the diode OFF-state, the −10 dB notch bandwidth centered around 5.3 GHz now shifts to 5.3 GHz radiating frequency after diode switching. For all diodes at the ON-state, simulated (using CST and ADS) and measured return losses are plotted in Fig. 7(b). It is observed from the return loss plot that the radiating bands have now switched in the stopband, and notch center frequency turns into radiating frequency. The F-shaped parasitic element designed at 5.3 GHz, now connected to the ground plane through metallic stabs by the mean of p-i-n diodes, vanishes all the radiations from rectangular patch and shifts the resonance at 5.3 GHz center frequency of the antenna structure. The differences between simulated and measured results observed other than 5.3 GHz can probably be attributed to imperfections of the components (five p-i-n diodes and five inductors), fabrication errors (over-etching) and fed wires for biasing of the diodes.

The simulated surface current distributions on the radiating patch and ground plane with all diodes in the OFF-state at different frequencies are presented in Fig. 8. As shown in Figs. 8(a)–(c), radiating frequencies are 4, 7 and 9 GHz, respectively. It is observed that the vertical and horizontal currents are more balanced at these frequencies. Fig. 8(d) shows that the surface current distribution at a center notch frequency of 5.3 GHz is mainly concentrated around the parasitic element. The currents are oppositely directed between the radiating edge of the rectangular patch and the edge of the parasitic element, resulting in the band-notched characteristics at 5.3 GHz center frequency, whereas with all diodes in the ON-state, the surface currents on the radiating edge and edge of the parasitic element are same in direction, which supports the radiation at 5.3 GHz, as depicted in Fig. 8(e).

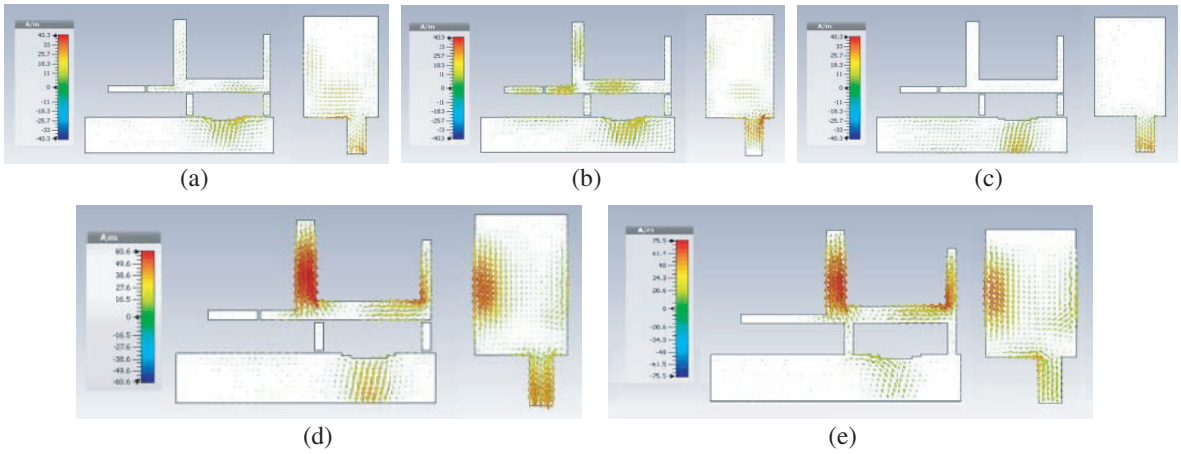

Figure 8. Simulated surface current distribution on the rectangular patch and the ground plane when all diodes are in the OFF-State (a) 4 GHz, (b) 7 GHz, (c) 9 GHz, (d) 5.3 GHz notch frequency. (e) 5.3 GHz when all diodes are in the ON-state.

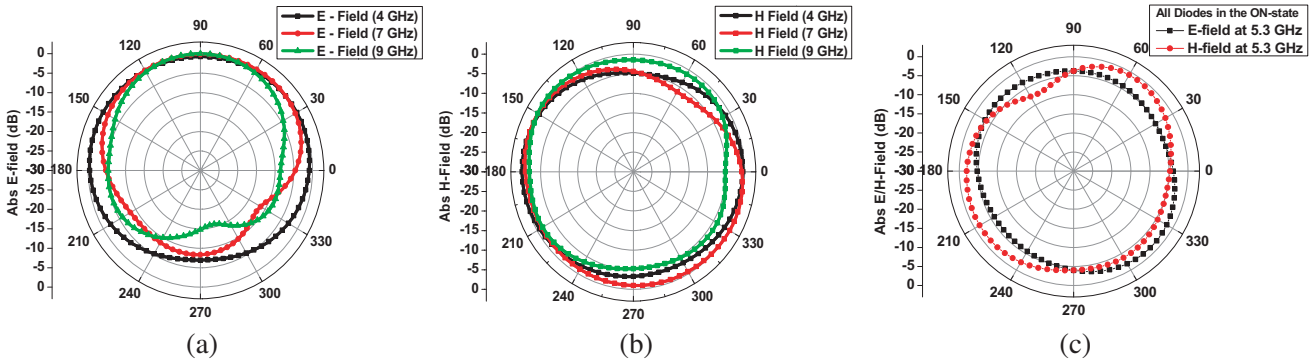

Figure 9. Measured 2D radiation pattern at 4 GHz, 7 GHz and 9 GHz when all diodes are in the OFF-state (a) E-plane, (b) H-plane, and at 5.3 GHz when all diodes are in the ON-state (c) E/H-Field.

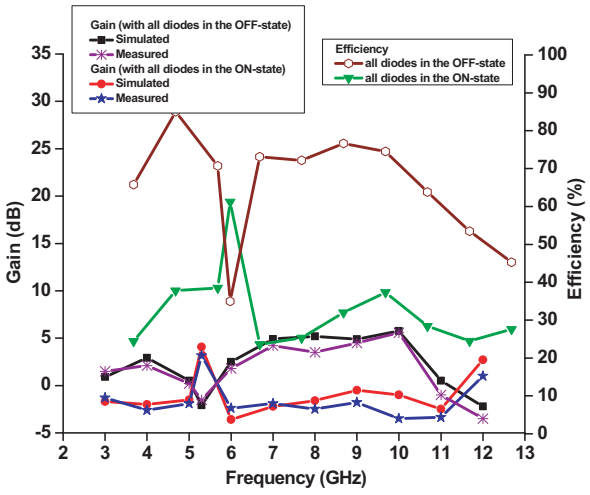

Figure 10. Comparison between the simulated and measured peak gain and measured efficiency of the proposed antenna when all diodes are in the OFF- and ON-state.

The measured E-plane and H-plane radiation patterns of the proposed antenna at 4, 7 and 9 GHz with all diodes in the OFF-state are displayed in Figs. 9(a)–(b), and that with all diodes in the ON-state at 5.3 GHz is shown in Fig. 9(c). In this state, it is observed that the antenna exhibits omnidirectional radiation characteristics at different operating frequencies. Fig. 10 displays the comparison between the simulated and measured peak gains of the proposed antenna with all the diodes in the OFF- and ON-states. With all the diodes in the OFF-state, it is observed that the antenna exhibits good gain over the entire operating band, except a drastic decrement at the notched 5.3 GHz center frequency band. In this state, the observed antenna gain varies between 2 to 6 dB at different operating frequencies. With all diodes in the ON-state, the proposed antenna radiates only at 5.3 GHz center frequency with approximately 4 dB gain. Good agreement between simulated and measured gains is observed. The measured efficiency of the antenna in the both states of the diodes is also shown in Fig. 10. It is observed that the efficiency of the antenna varies from 65 to 85% for the radiating bands, with all diodes in the OFF-state. With all diode in the ON-state, maximum efficiency of 60% is achieved at 5.3 GHz.

4. CONCLUSIONS

A frequency reconfigurable antenna with switchable notch characteristics at 5.3 GHz center frequency has been demonstrated successfully for the first time. By inserting an F-shaped parasitic element and three stubs on the ground plane, a UWB antenna with band rejection characteristics can be obtained. Five p-i-n diodes are used to switch 5.3 GHz center frequency band. The proposed antenna with all the diodes in the OFF-state results in the UWB antenna radiating from 3.3 to 10.3 GHz with 4.9 to 5.7 GHz band-notched characteristics. With all the diodes in the ON-state, the proposed antenna radiates at center frequency of 5.3 GHz in the WLAN frequency band. For both cases of diodes in the ON- and OFF-states, the simulated and measured results are compared, and a good agreement is observed.

REFERENCES

1. US Federal Communications Commission, et al., "FCC revision of part 15 of the commission's rules regarding ultra-wideband transmission systems: First report and order," *Technical Report*, Feb. 2002.
2. Gheethan, A. A. and D. E. Anagnostou, "Dual band-reject UWB antenna with sharp rejection of narrow and closely-spaced bands," *IEEE Trans. Antennas Propag.*, Vol. 60, No. 4, 2071–2076, Apr. 2012.
3. Khidre, A., F. Yang, and A. Z. Elsherbeni, "Patch antenna with a varactor-loaded slot for reconfigurable dual-band operation," *IEEE Trans. Antennas Propag.*, Vol. 63, No. 2, 755–760, Feb. 2015.
4. Trad, I. B., J. M. Floch, H. Rmili, L. Laadhar, and M. Drissi, "Planar elliptic broadband antenna with wide range reconfigurable narrow notched bands for multi-standard wireless communication devices," *Progress In Electromagnetics Research*, Vol. 145, 69–80, Feb. 2014.
5. Qui, P. Y., F. Wei, and Y. J. Guo, "Wideband-to-narrowband tunable antenna using a reconfigurable filter," *IEEE Trans. Antennas Propag.*, Vol. 63, No. 5, 2282–2285, May 2015.
6. Al-Zayed, A. S., M. A. Kourah, and S. F. Mahmoud, "Frequency-reconfigurable single and dual-band designs of a multi-mode microstrip antenna," *IET Microw. Antennas Propag.*, Vol. 8, No. 13, 1105–1112, May 2014.
7. Tariq, A. and H. G. Shiraz, "Frequency-reconfigurable monopole antennas," *IEEE Trans. Antennas Propag.*, Vol. 60, No. 1, 44–50, Jan. 2012.
8. Valizade, A., C. Ghobadi, J. Nourinia, and M. Ojaroudi, "A novel design of reconfigurable slot antenna with switchable band notch and multiresonance functions for UWB applications," *IEEE Antennas Wireless Propag. Lett.*, Vol. 11, 1166–1169, Oct. 2012.
9. Ali, W. A. E. and R. M. A. Moniem, "Frequency reconfigurable triple band-notched ultra-wideband antenna with compact size," *Progress In Electromagnetics Research C*, Vol. 73, 37–46, Apr. 2017.

10. Anagnostou, D. E., M. T. Chryssomallis, B. D. Braaten, J. L. Ebel, and N. Sepúlveda, "Reconfigurable UWB antenna with RF-MEMS for on-demand WLAN rejection," *IEEE Trans. Antennas Propag.*, Vol. 62, No. 2, 602–608, Feb. 2014.
11. Nikolaou, S., N. D. Kingsley, G. E. Ponchak, J. Papapolymerou, and M. M. Tentzeris, "UWB elliptical monopoles with a reconfigurable band notch using MEMS switches actuated without bias lines," *IEEE Trans. Antennas Propag.*, Vol. 57, No. 8, 2242–2251, Aug. 2009.
12. Loizeau, S. and A. Sibille, "Reconfigurable ultra-wideband monopole antenna with a continuously tunable band notch," *IET Microw. Antennas Propag.*, Vol. 8, No. 5, 346–350, Oct. 2013.
13. Badamchi, B., J. Nourinia, C. Ghobadi, and A. V. Shahmirzadi, "Design of compact reconfigurable ultra-wideband slot antenna with switchable single/dual band notch functions," *IET Microw. Antennas Propag.*, Vol. 8, No. 8, 541–548, Nov. 2013.
14. Kurra, L., M. P. Abegaonkar, A. Basu, and S. K. Koul, "Switchable and tunable notch in ultra-wideband filter using electromagnetic bandgap structure," *IEEE Microwave Wireless Propag. Lett.*, Vol. 24, No. 12, 839–841, Dec. 2014.
15. Gupta, K. C., R. Garg, I. J. Bhal, and P. Bhartia, *Microstrip Lines and Slotlines*, 2nd Edition, 10–15, Artech House, 1996.
16. Kumar, G. and K. P. Ray, *Broadband Microstrip Antennas*, 362–368, Artech House, 2003.
17. Available at http://www.cst.com.
18. Rostamzadeh, M., S. Mohamadi, J. Nourinia, C. Ghobadi, and M. Ojaroudi, "Square monopole antenna for UWB applications with novel rod-shaped parasitic structures and novel v-shaped slots in the ground plane," *IEEE Antenna Wireless Propag. Lett.*, Vol. 11, 446–449, Mar. 2013.
19. Fereidoony, F., S. Chamaani, and S. A. Mirtaheri, "Systematic design of UWB monopole antenna with stable omnidirectional radiation pattern," *IEEE Antennas Wireless Propag. Lett.*, Vol. 11, 752–755, Jul. 2012.
20. Data sheet at https://cdn.macom.com/datasheets/MA4SPS402.pdf.